

PROCEEDINGS OF SPIE

[SPIDigitalLibrary.org/conference-proceedings-of-spie](https://spiedigitallibrary.org/conference-proceedings-of-spie)

Automated segmentation of oblique abdominal muscle based on body cavity segmentation in torso CT images using U-Net

Kamiya, N., Zhou, X., Kato, H., Hara, T., Fujita, H.

N. Kamiya, X. Zhou, H. Kato, T. Hara, H. Fujita, "Automated segmentation of oblique abdominal muscle based on body cavity segmentation in torso CT images using U-Net," Proc. SPIE 12177, International Workshop on Advanced Imaging Technology (IWAIT) 2022, 121771V (30 April 2022); doi: 10.1117/12.2624316

SPIE.

Event: International Workshop on Advanced Imaging Technology 2022 (IWAIT 2022), 2022, Hong Kong, China

Automated segmentation of oblique abdominal muscle based on body cavity segmentation in torso CT images using U-Net

N. Kamiya^{*a}, X. Zhou^b, H. Kato^c, T. Hara^{b, d}, H. Fujita^b

^aSchool of Information Science and Technology, Aichi Prefectural University, 1522-3 Ibaragabasama, Nagakute, Aichi, JAPAN 480-1198; ^bFaculty of Engineering, Gifu University, 1-1 Yanagido, Gifu, Gifu, JAPAN 501-1194, ^cDepartment of Radiology, Graduate School of Medicine, Gifu University, 1-1 Yanagido, Gifu, Gifu, JAPAN 501-1194, ^dCenter for Healthcare Information Technology (C-HiT), Tokai National Higher Education and Research System, Aichi, JAPAN 464-8601

ABSTRACT

The body cavity region contains organs and is an essential region for skeletal muscle segmentation. This study proposes a method to segment body cavity regions using U-Net with focus on the oblique abdominal muscles. The proposed method comprises two steps. First, the body cavity is segmented using U-Net. Subsequently, the abdominal muscles are identified using recognition techniques. This is achieved by removing the segmented body cavity region from the original computerized tomography (CT) images to obtain a simplified CT image for training. In this image, the visceral organ regions are masked by the body cavity, ensuring that the organs therein are excluded from the segmentation target in advance, which has been a primary concern in the conventional method of skeletal muscle segmentation. The segmentation accuracies of the body cavity and oblique abdominal muscle in 16 cases were 98.50% and 84.89%, respectively, in terms of the average Dice value. Furthermore, it was observed that body cavity information reduced the number of over-extracted pixels by 36.21% in the segmentation of the oblique abdominal muscles adjacent to the body cavity, improving the segmentation accuracy. In future studies, it could be beneficial to examine whether the proposed simplification of CT images by segmentation of body cavities is also effective for abdominal musculoskeletal muscles adjacent to body cavities divided by tendon ends, such as the rectus abdominis.

Keywords: Body Cavity, Oblique Abdominal Muscle, U-Net, Segmentation, CT images

1. INTRODUCTION

Skeletal muscle segmentation in the computerized tomography (CT) images of the torso is challenging because of over-extraction in the body cavity region [1]. We focused on the body cavity region because it contains many organs and is bordered by the skeletal muscles on its surface. The abdominal oblique muscle, which is the target of this study, is difficult to segment because its CT images are comparable to those of the liver and intestine regions in the inner abdominal cavity. Other skeletal muscle segmentation studies in CT images include skeletal muscle segmentation in the hip and thigh by Hiasa et al. [2], in thoracic and lumbar spine axial slices by Setareh et al. [3], and in the third lumbar vertebra (L3) section by Castiglione et al. [4]. Hiasa et al. achieved automatic segmentation of 19 skeletal muscles in the hip and thigh using Bayesian U-Net. It recognized 19 types of skeletal muscles for 20 test cases with an average Dice value of 89% [2]. Setareh et al. used a two-branch network with two learning steps to segment skeletal muscles from axial images of the fourth thoracic vertebra (T4) and L3 in CT images and achieved an average accuracy of 0.96 Jaccard coefficient [3]. Castiglione et al. developed two sets of U-Net-based models to identify the L3 level in the sagittal plane and segment the skeletal muscles as a single region in the corresponding axial cross-sectional images, achieving an average accuracy of 93% Dice value for 74 cases [4]. These studies have shown high segmentation accuracy for skeletal muscle, but there are no organs in the lower thighs or the L3 or T4 regions with CT images similar to that of skeletal muscle. Therefore, these studies considered neither the necessity nor the difficulty of discriminating between organ tissue regions in abdominal skeletal muscle segmentation. In addition, the studies by Setareh et al. and Castiglione et al. are based on two-dimensional cross-sectional segmentation of vertebral bodies; three-dimensional skeletal muscle segmentation was not achieved.

*n-kamiya@ist.aichi-pu.ac.jp; phone 81 561 76-8770; fax 81 561 64-1108; <http://www.ist.aichi-pu.ac.jp/~n-kamiya/>
This work was supported in part by the JSPS Grant-in-Aid for Scientific Research (C) (#21K12731).

Accordingly, we proposed a segmentation method for body cavities in CT images and automated segmentation of abdominal muscles based on segmented body cavity regions. In this study, we investigated the possibility of using the body cavity region as prior information for skeletal muscle segmentation around this region by using it to segment the oblique abdominal muscle, which is a skeletal muscle adjacent to it.

2. METHODS

A schematic of the proposed method is shown in Fig. 1. The proposed method consists of two steps: Step 1 for body cavity segmentation using U-Net, and Step 2 for abdominal muscle recognition using a simplified CT image for training by removing the segmented body cavity region from the original CT images.

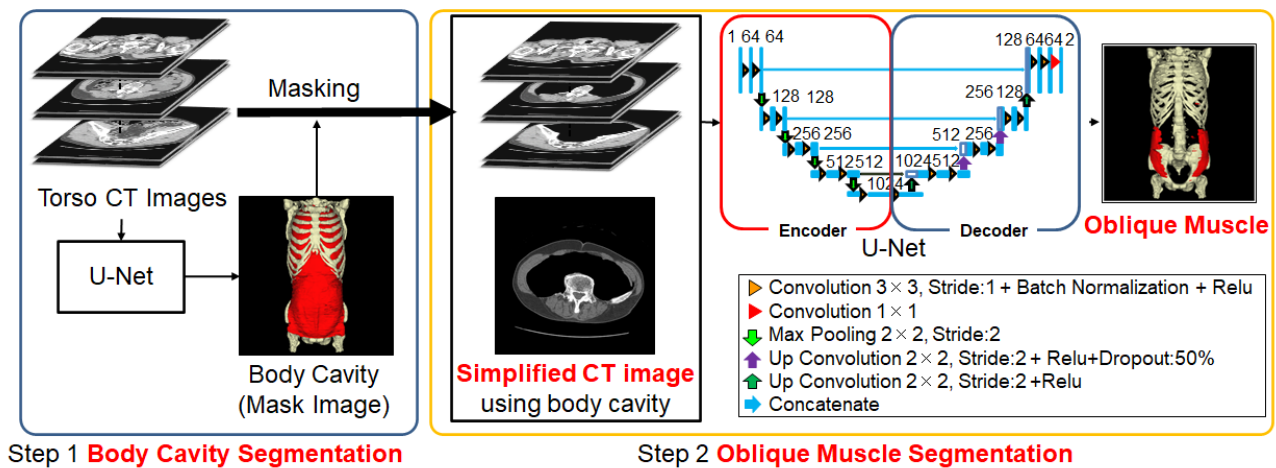


Figure 1. Overview of body cavity segmentation (Step 1) and oblique abdominal muscle segmentation (Step 2) using simplified CT images with body cavities.

2.1 Body cavity segmentation

In step 1, we used 2D U-Net, one of the models of deep learning (DL) networks, to automatically segment body cavity regions from torso CT images. First, we performed data augmentation on the CT and ground-truth images, employing horizontal and vertical translation, rotation, scaling, shear transformation, and left-right flipping. The parameters for these were the same as those used by Hiasa et al. in their augmentation method for skeletal muscle segmentation [2]. The parameters are as follows: horizontal and vertical translation: from -25% to +25% of the matrix; rotation: from -10° to $+10^\circ$; scaling: a random value from 0.65 to 1.35 times the length of one side, keeping the aspect ratio of the image constant, and shear transformation from -35° to $+35^\circ$. Here, the pixel value of the region without a corresponding pixel in the pre-processing image was assumed to be the lowest pixel value of the background. The training data can be doubled by randomly applying these methods. Then, the CT and ground-truth images were input to the U-Net for training. Following this, we automatically segmented the body cavities from the CT images using the weights obtained from the training. In this study, batch normalization [6] and dropout were added to the base U-Net [5] to suppress overfitting. Here, batch normalization was inserted in the succeeding layer of each convolution layer, and dropout was added to the second and third layers of the decoder. The probability of dropout was 0.5, as was the case in the study of the dropout technique [7] by Srivastava et al. As a post-processing step, because the body cavity is a large region containing the organs in the thoracic, abdominal, and pelvic cavities, we performed a 3D labeling process and defined the region with the largest volume as the body cavity. The training parameters of this network were as follows: the number of epochs was 50, the batch size was 10, the optimization function was Adam, the learning rate was 1×10^{-4} , and the loss function was a 1 - Dice loss.

2.2 Oblique muscle segmentation

The U-Net architecture for the segmentation of the abdominal oblique muscle was the same as that for the segmentation of the body cavity in Step 1, as were its training parameters. In Step 2, to train U-Net for the segmentation of the abdominal oblique muscle, a masking process was applied to the torso CT image using the segmented body cavity region, the visibility of which was set to 0 to create a simplified CT image. In this simplified CT image, the visceral organ regions are masked by the body cavity, precluding them from the segmentation target in advance. This solves the primary issue in conventional

methods of skeletal muscle segmentation. An example of the original image and a simplified CT image are shown in Fig. 2. It can be seen that the region of the abdominal oblique muscle is preserved, and the region of the adjacent organ i.e., the intestines is masked.

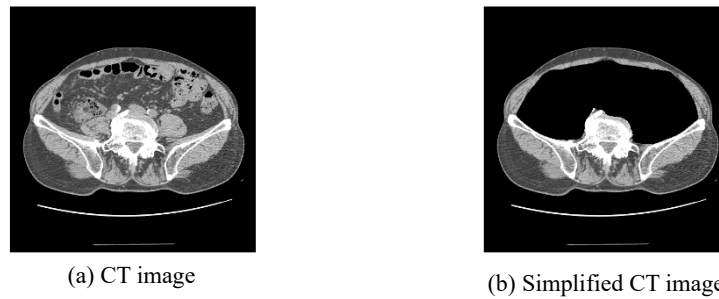


Figure 2. Example of the original image and a simplified CT image.

3. EXPERIMENTS

In this study, we used 16 non-contrast torso CT images obtained using the LightSpeed Ultra 16 (GE Healthcare, Chicago, IL, USA) at Gifu University Hospital. The image size was $512 \times 512 \times 849-1031$ [voxel], and the spatial resolution was $0.625 \text{ mm} \times 0.625 \text{ mm} \times 0.625 \text{ mm}$. CT images were divided into 10, 2, and 4 cases in the training, validation, and test sets, respectively. The segmentation accuracy was verified by the Dice, recall, and precision rate using 4-fold cross-validation. The Dice rate was used to evaluate the overall segmentation accuracy, including under-extracted and over-extracted pixels, the recall rate was used to evaluate under-extracted pixels, and the precision value was used to evaluate over-extracted pixels. The definitions of these metrics are as follows.

$$\text{Dice} = \frac{2 \times |A \cap B|}{|A| + |B|} \quad (1)$$

$$\text{Recall} = \frac{|A \cap B|}{|A|} \quad (2)$$

$$\text{Precision} = \frac{|A \cap B|}{|B|} \quad (3)$$

where A refers to the ground truth, B refers to the segmentation result, and operator $||$ returns the number of voxels contained in the region.

Ground truth was created by manual segmentation of the body cavity and oblique abdominal muscle, as recommended by an anatomist. In this study, we defined the ground truth as the body cavity region that includes the deep muscles of the psoas major and iliacus regions. This was primarily to counter the effect of over-extraction of intracorporeal organ tissues in superficial skeletal muscle segmentation. Similarly, the region including the three muscle groups, viz., the external oblique abdominal muscle, internal oblique abdominal muscle, and transverse abdominal muscle adjacent to the abdominal cavity in the slice below the lowest rib is defined as the grand trunk of the oblique abdominal muscle in this study.

The experiments were conducted on a computer with 4 Tesla V100 (32 GB) graphics processing units (GPUs). We employed TensorFlow-GPU 1.15.0 and Keras 2.2.5 as machine-learning libraries.

4. RESULTS

Table 1 presents the evaluation results of body cavity segmentation that was undertaken. The mean dice value of the segmentation results was 0.985 (standard deviation [SD]: 0.004), the mean recall was 0.983 (SD: 0.006), and the mean precision was 0.987 (SD: 0.007). The 3D-rendered images of the body cavity segmentation are shown in Fig. 3. The overlapping area between the segmentation result and the ground truth is marked in yellow, the over-extracted area in red, and the under-extracted area in green.

Table 1. Body cavity segmentation results by 4-fold cross-validation (mean \pm standard deviation) [%].

	Dice	Recall	Precision
1st	98.71 \pm 0.22	98.49 \pm 0.25	98.94 \pm 0.44

2nd	98.40 ± 0.54	98.75 ± 0.19	98.06 ± 0.95
3rd	98.31 ± 0.44	97.78 ± 0.80	98.85 ± 0.19
4th	98.57 ± 0.25	98.26 ± 0.34	98.87 ± 0.23
Average	98.50 ± 0.42	98.32 ± 0.58	98.68 ± 0.65

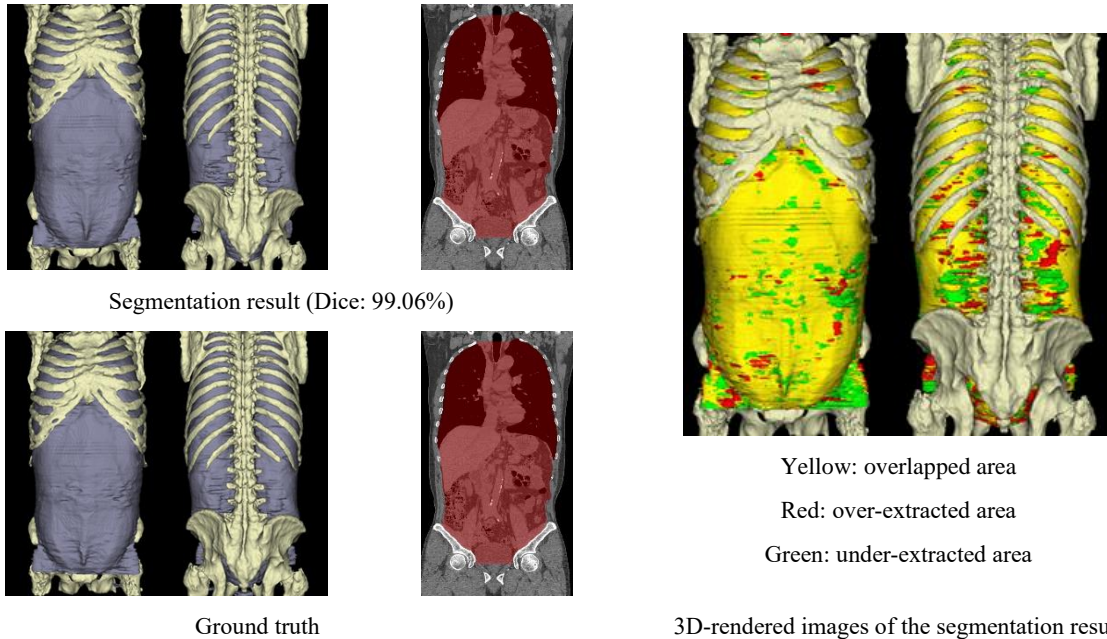


Figure 3. Segmentation results and 3D-rendered images of the body cavity region.

Table 2 shows the evaluation results of the oblique abdominal muscle segmentation conducted using the proposed body cavity segmentation method and without it. The mean Dice value of the segmentation results using the proposed method was 0.849 (SD: 0.081), the mean recall was 0.805 (SD: 0.120), and the mean precision was 0.908 (SD: 0.047). In contrast, the mean Dice value of the segmentation results without body cavity segmentation was 0.819 (SD: 0.073), the mean recall was 0.762 (SD: 0.119), and the mean precision was 0.902 (SD: 0.041). The number of over-extracted pixels decreased from 7 120 967 without body cavity segmentation to 4 906 455 using the body cavity segmentation method. In particular, the number of over-extracted pixels in the body cavity region decreased from 5 033 506 to 3 210 958, which is a 36% decrease.

Table 2. Oblique abdominal muscle segmentation results by 4-fold cross-validation (mean ± standard deviation) [%].

	Dice	Recall	Precision	Over-extracted pixels	Over-extracted pixels (body cavity)
w/o body cavity	81.93 ± 7.25	76.22 ± 11.85	90.16 ± 4.06	7 120 967	5 033 506
w/ (proposed)	84.89 ± 8.06	80.53 ± 12.04	90.80 ± 4.68	4 906 455	3 210 958

Figure 4 shows the segmentation results and 3D-rendered image of the oblique abdominal muscles. Figure 4(a) shows the results without body cavity segmentation, and 4(b) shows the results with body cavity segmentation. The blue arrows indicate intestinal regions that were over-extracted using the method without body cavity segmentation. This shows that body cavity segmentation suppresses over-extraction of pixels of the intestinal area in oblique abdominal segmentation.

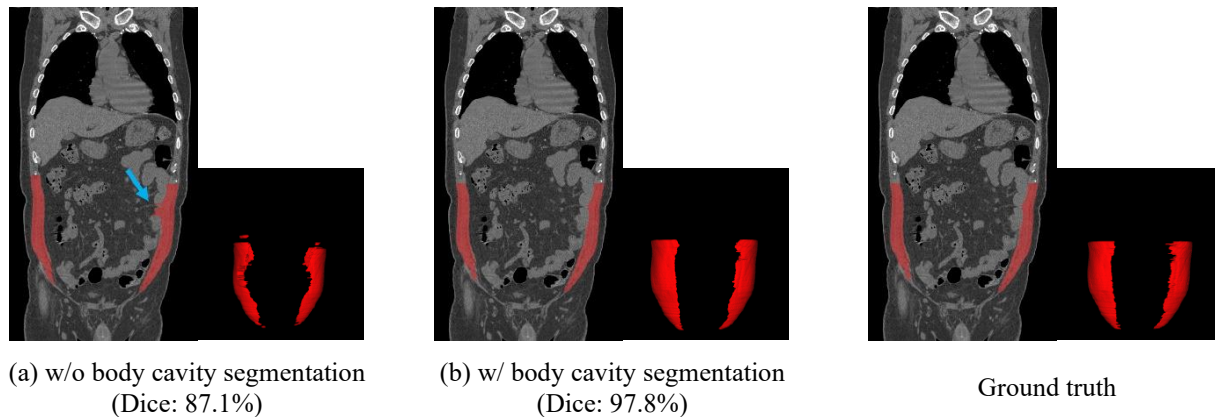


Figure 4. Segmentation results and 3D-rendered images of the oblique abdominal muscles. (a) shows the results without body cavity segmentation, and (b) shows the results with body cavity segmentation.

5. DISCUSSIONS

As described in section 4, the segmentation results of the body cavity were good, with an average Dice value of 98.5% based on the four-part cross-validation. However, in the visual evaluation, certain high-intensity regions except the skeleton in the visceral regions of the body cavity remained unsegmented. As the CT characteristics of these high-intensity regions were identical to those of the skeletal regions, it was assumed that these high-intensity regions were not extracted because they were recognized as skeletal regions that were excluded from the body cavity regions during prediction. Similarly, over-extraction of the body cavity occurred in cases where the body surface area possessed an appearance different from that of the normal structure. Figure 5 shows a case in which the body cavity was not extracted in a high-intensity region (arrow) and a case in which the body cavity was over-extracted in a case in which the body surface appeared different from the normal structure (arrow). The upper figure shows the segmentation results, and the lower figure shows the ground truth.

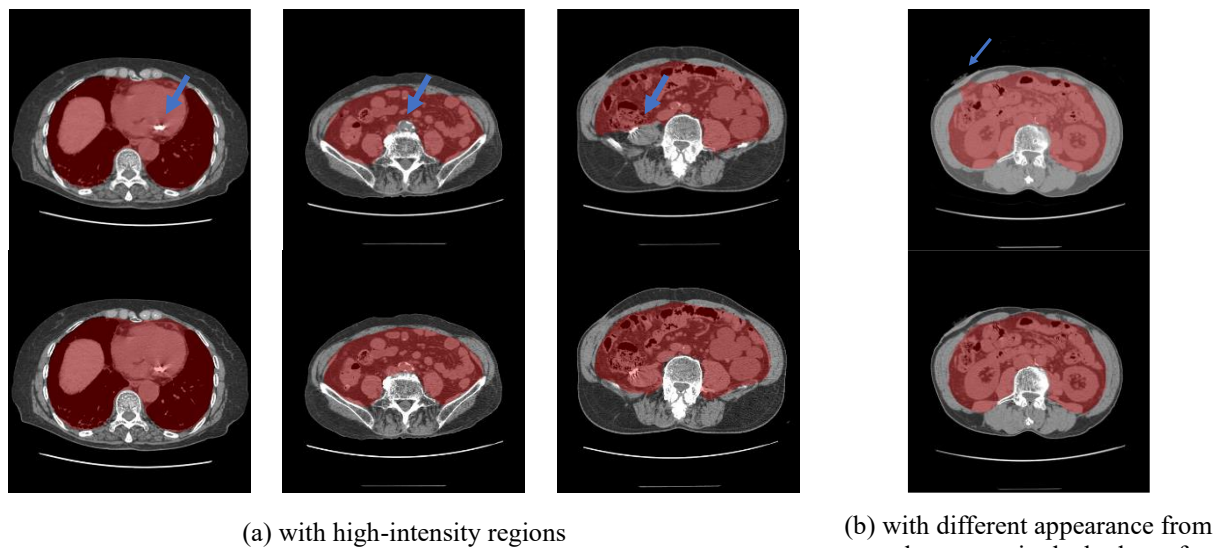


Figure 5. Under-extracted region in the high-intensity region (arrow) and over-extracted region in the body surface area with different appearance (arrow) from normal structure (upper: segmentation result, lower: ground truth)

The accuracy of the segmentation of the oblique abdominal muscle was 84.89% with the proposed method, using CT images simplified by segmentation in the body cavity region. In terms of the improvement of the segmentation accuracy of the oblique abdominal muscle, the over-extraction was suppressed by 31.10% on average and by 36.21% in the body cavity region, as shown in Table 2. In particular, over-extraction was reduced in 13 of the 16 cases, and in 14 of the 16 cases, over-extraction in the body cavity region was suppressed. Thus, the over-extraction was suppressed because the

body cavity region was masked in the simplified CT images by segmentation of the body cavity region, and the visceral region information, which has a similar shading distribution of CT values to skeletal muscle, could be distinguished. This shows the possibility of using body cavity information as prior information in the segmentation of skeletal muscles or organs. However, certain limitations have to be overcome, such as those in the cases with high-intensity regions with CT values similar to those of bones and those in the cases of body surface structures that differ from normal structures, as shown in Figure 5.

It is unclear whether this can be solved by increasing the number of training data or upgrading the DL network. In this study, it is noteworthy that the proposed method performed well on a limited dataset of 16 cases and was able to automatically segment the oblique abdominal muscles in three dimensions, which had not been achieved in previous studies [3-4]. We found that prior information about the body cavity was effective in suppressing overextraction of skeletal muscles, but localization using the skeletal muscle attachment bones [8] should also be considered when considering site-specific segmentation of skeletal muscles.

6. CONCLUSIONS

We proposed a method for body cavity segmentation in CT images and automated segmentation of oblique abdominal muscles based on segmented body cavity regions. As a result, the segmentation accuracy of the body cavity and oblique abdominal muscle in 16 cases were 98.50% and 84.89%, respectively, in terms of the average Dice value. Furthermore, it was found that body cavity information suppressed the number of over-extracted pixels by 36.21% in the segmentation of the oblique abdominal muscles adjacent to the body cavity and improved the segmentation accuracy. However, segmentation was not successful in two scenarios. One was the case of high-intensity regions with characteristics similar to the skeleton and the other was the case of body surface regions with abnormal structure. In the first scenario, the region remained unsegmented, and in the latter, it was over-extracted. Nevertheless, the proposed simplification of CT images by segmentation of body cavities has significant potential scope for future studies. The results obtained in this study suggest that the proposed method can be extended to the segmentation of abdominal musculoskeletal muscles adjacent to body cavities divided by tendon ends, such as the rectus abdominis.

REFERENCES

- [1] Kamiya, N., Oshima, A., Zhou, X., Kato, H., Hara, T., Miyoshi, T., Matsuo, M. and Fujita, H., "Surface muscle segmentation using 3d u-net based on selective voxel patch generation in whole-body CT images," *Appl. Sci.* 10(13), 4477 (2020).
- [2] Hiasa, Y., Otake, Y., Takao, M., Ogawa, T., Sugano, T. and Sato, Y., "Automated muscle segmentation from clinical CT using Bayesian U-net for personalized musculoskeletal modeling," *IEEE Trans. Med. Imaging* 39(4), 1030-1040 (2019).
- [3] Dabiri, S., Popuri, K., Felicaano, E., Elizabeth, C., Caan, B. and Baracos, V., "Muscle segmentation in axial computed tomography (CT) images at the lumbar (L3) and thoracic (T4) levels for body composition analysis," *Comput. Med. Imaging Graph.* 75, 47-55 (2019).
- [4] Castiglione, J., Somasundaram, E., Gilligan, L. A., Trout, A. T. and Brady, S., "Automated segmentation of abdominal skeletal muscle on pediatric CT scans using deep learning," *Radiology: Artificial Intelligence* 3(2), e200130 (2021).
- [5] Ronneberger, O., Fischer, P. and Brox, T., "U-Net: Convolutional networks for biomedical image segmentation," *Proc. Medical Image Computing and Computer Assisted Intervention* 459, 234-241 (2015).
- [6] Ioffe, S. and Szegedy, C., "Batch normalization: Accelerating deep network training by reducing internal covariate shift," *Proc. the 32nd International Conference on Machine Learning*, 448-456 (2015).
- [7] Srivastava, N., Hinton, G., Krizhevsky, A., Sutskever, I. and Salakhutdinov, R., "Dropout: A simple way to prevent neural networks from overfitting," *J Mach. Learn. Res.* 15(1), 1929-1958 (2014).
- [8] Wakamatsu, Y., Kamiya, N., Zhou, X., Kato, H., Hara, T., and Fujita, H., "Automatic segmentation of supraspinatus muscle via bone-based localization in torso computed tomography images using U-Net," *IEEE Access.* 9, 155555-155563 (2021).